Insect Biochemistry and Molecular Biology 104 (2019) 30–38

Contents lists available at ScienceDirect

Insect Biochemistry and Molecular Biology

journal homepage: www.elsevier.com/locate/ibmb

Two CCCH-type zinc finger domains in the Masc protein are dispensable for masculinization and dosage compensation in *Bombyx mori*

Takashi Kiuchi*, Yudai Sugano, Toru Shimada, Susumu Katsuma**

Department of Agricultural and Environmental Biology, Graduate School of Agricultural and Life Sciences, The University of Tokyo, Yayoi 1-1-1, Bunkyo-ku, Tokyo, 113-8657, Japan

ARTICLE INFO

Keywords:
Bombyx mori
CRISPR/Cas9
Dosage compensation
Sex determination
Zinc finger domains

ABSTRACT

The *Masculinizer* (*Masc*) gene encodes a novel lepidopteran-specific protein that controls both masculinization and dosage compensation in the silkworm *Bombyx mori*. The Masc protein possesses two CCCH-type zinc finger domains (ZFs), a nuclear localization signal, and an 11-amino-acid region that is highly conserved among lepidopteran insects. Using a cell-based assay system, we revealed that two cysteine residues localized in the conserved region, but not ZFs, are required for masculinization. In addition, nuclear localization of the Masc protein is not associated with masculinizing activity. Because dosage compensation is considered to occur in the nucleus, we inferred that the two ZFs play a role in the establishment of dosage compensation. To investigate this hypothesis at the organism level, we utilized the CRISPR/Cas9 system and established three *B. mori* strains whose *Masc* is partially deleted at different regions. The strain lacking the 210 C-terminal amino acids of the Masc protein showed male-specific embryonic lethality due to its low abundance and/or instability. The male embryos of this strain expressed the female-type splice variants of *B. mori doublesex* and did not express the male-type mRNA of *B. mori IGF-II mRNA-binding protein*. Furthermore, mRNA levels of Z-linked genes were abnormally enhanced only in male embryos. In contrast, the strain lacking both ZFs grew normally and did not show any defective phenotypes including sexual differentiation and the expression of Z-linked genes, demonstrating that the two CCCH-type ZFs, which are conserved in lepidopteran Masc homologs, are dispensable for masculinization and dosage compensation.

1. Introduction

The female heterogamety system is observed in a diverse range of animals including butterflies and moths. In the silkworm *Bombyx mori*, females have WZ sex chromosomes, whereas males have two Z sex chromosomes (Tanaka, 1916). Genetic studies using mutant *B. mori* strains have revealed that one copy of the W chromosome is sufficient for determining *B. mori* femaleness, regardless of the copy number of the Z chromosome (Hasimoto, 1933), indicating that the W chromosome encodes a dominant feminizing gene (*Feminizer*, *Fem*). In 2014, we adopted an approach based on RNA-sequencing (RNA-seq) of male and female embryonic RNAs and succeeded in identifying a feminizing factor, *Fem* (Kiuchi et al., 2014). *Fem* RNA is transcribed from the W chromosome and produces female-specific PIWI-interacting RNA (piRNA). We also found that *Fem* piRNA forms a complex with Siwi, one of the *B. mori* PIWI proteins, and that this complex targets a protein-coding mRNA expressed from the Z chromosome. Embryonic knockdown of this Z-linked gene resulted in feminization of male embryos, indicating that this gene encodes a masculinizing factor, and we thus named it *Masculinizer* (*Masc*). We and Xu et al. elucidated the masculinizing activity *in vivo* by overexpression and CRISPR/Cas9-mediated somatic mutation of the *Masc* gene using transgenic silkworms, respectively (Sakai et al., 2016; Xu et al., 2017). Furthermore, we also revealed that embryonic knockdown of *Masc* mRNA resulted in male-specific death, which was caused by a failure of dosage compensation (Kiuchi et al., 2014). These findings indicate that the Masc protein controls not only masculinization but also dosage compensation in *B. mori*.

Abbreviations: Masc, *Masculinizer*; ZFs, zinc finger domains; *Fem*, *Feminizer*; RNA-seq, RNA-sequencing; piRNA, PIWI-interacting RNA; *Bmdsx*, *B. mori doublesex*; *BmIMP*, *B. mori IGF-II mRNA-binding protein*; EGFP, enhanced green fluorescent protein; NLS, nuclear localization signal; sgRNA, synthetic guide RNA; T7ENI, T7 endonuclease I; Masc-R, *Fem* piRNA-resistant Masc; M1, NIAS-Bm-M1; HotSHOT, hot sodium hydroxide and tris; RT-qPCR, quantitative reverse transcription-PCR

* Corresponding author.
** Corresponding author.
E-mail addresses: kiuchi@ss.ab.a.u-tokyo.ac.jp (T. Kiuchi), katsuma@ss.ab.a.u-tokyo.ac.jp (S. Katsuma).

https://doi.org/10.1016/j.ibmb.2018.12.003
Received 7 September 2018; Received in revised form 4 December 2018; Accepted 6 December 2018
Available online 07 December 2018
0965-1748/

Masc is a CCCH-tandem zinc finger (ZF) protein that is conserved among lepidopteran insects (Kiuchi et al., 2014). To identify the regions required for the masculinizing activity of the *B. mori* Masc protein, we established a transient assay system using the *B. mori* BmN-4 cell line (Katsuma et al., 2015). As BmN-4 is derived from *B. mori* ovary, the splicing pattern of *B. mori doublesex* (*Bmdsx*), a gene that acts at the end of the sex differentiation cascade, is the female type ($Bmdsx^F$) (Suzuki et al., 2003, 2005). We found that transfection of *Masc* cDNA into BmN-4 cells resulted in production of the male-type splice variant of *Bmdsx* ($Bmdsx^M$) (Kiuchi et al., 2014). Moreover, *Masc* overexpression in BmN-4 cells induces transcriptional increase in the male-type mRNA of *B. mori IGF-II mRNA-binding protein* ($BmIMP^M$) (Fukui et al., 2015; Katsuma et al., 2015; Lee et al., 2015), the product of which plays a role in the male-specific splicing of *Bmdsx* (Suzuki et al., 2010). Using this artificial system, we successfully identified the regions and amino acid residues required for the masculinizing activity of the Masc protein; two cysteines at residues 301 and 304, both of which are completely conserved among lepidopteran Masc homologs, are required for the masculinizing activity (Katsuma et al., 2015). On the other hand, deletion of two ZFs did not affect the mRNA levels of $Bmdsx^M$ and $BmIMP^M$; thus, the role of the CCCH ZFs in Masc functions remains unclear.

Dosage compensation is generally considered to occur in the nucleus, so the Masc protein should function there. Using a series of Masc derivatives fused to enhanced green fluorescent protein (EGFP), we showed that Masc exhibits distinct nuclear localization and that there is a strong determinant of this localization between residues 200 and 300 of the Masc protein (Sugano et al., 2016). Further experiments identified a bipartite nuclear localization signal (NLS) that is located between residues 274 and 290 (Sugano et al., 2016). Intriguingly, a Masc derivative that is localized in the cytoplasm also induced the expression of both $Bmdsx^M$ and $BmIMP^M$, showing that nuclear localization of the Masc protein is not required for its masculinizing activity (Sugano et al., 2016). Considering the fact that some CCCH-tandem ZF-containing proteins play biological roles by binding nucleic acids via their ZFs (Blackshear and Perera, 2014; Brooks and Blackshear, 2013; Pomeranz et al., 2010), it is likely that the Masc ZFs bind genomic DNA or RNA in the nucleus to establish dosage compensation in *B. mori* males.

As *B. mori* cultured cell lines possess abnormal numbers of chromosomes (Imanishi and Ohtsuki, 1988), it is quite challenging to establish a cell-based assay system for evaluating the gene dosage effects. To overcome this issue, it is necessary to establish an organism-based *in vivo* assay system for dosage compensation. Recently, the CRISPR/Cas9 system has been applied to gene knockout studies on insects including *B. mori* (Wang et al., 2013; Daimon et al., 2014; Ma et al., 2014; Wei et al., 2014). In this study, we generated several *Masc* mutant *B. mori* strains by the CRISPR/Cas9 system and characterized their phenotypes in detail. The results clearly showed that deletion of the 210 C-terminal amino acids caused distinct defects in both dosage compensation and sexual differentiation, whereas, unexpectedly, two ZFs are dispensable for both functions.

2. Materials and methods

2.1. Silkworm strains

The non-diapause strain N4 maintained in our laboratory was used in this study. All larvae were fed with fresh mulberry leaves or artificial diet SilkMate (NOSAN) under a continuous cycle of 12 h light and 12 h darkness at 25 °C. The mutant strain ΔC210 was maintained by crossing between a mutant female (−/W) and a male carrying heterozygous mutation (−/+) because the homozygous mutation (−/−) was embryonic lethal in males (Fig. 4A, B, E).

2.2. CRISPR/Cas9-mediated mutagenesis

We prepared synthetic guide RNAs (sgRNAs) and *Cas9* mRNA according to a method reported previously (Bassett et al., 2013). Specific sgRNA target sequences were searched using ZiFiT Targeter (Sander et al., 2010; Hwang et al., 2013). Primers used for sgRNA transcription *in vitro* are listed in Supplemental Table S1. The plasmid MLM3613 (Addgene) was used for *Cas9* mRNA synthesis *in vitro*. A mixture of sgRNA (0.5 μg) and *Cas9* mRNA (10 μg) in a 30 μl volume of RNase-free water with 1.5 μl of 3 M sodium acetate (pH 5.2) was added into 90 μl of ethanol and centrifuged for RNA precipitation. The pelleted RNA was washed twice with 70% ethanol and resuspended in 11 μl of the injection buffer (100 mM KOAc, 2 mM $Mg(OAc)_2$, 30 mM HEPES-KOH; pH 7.4). The RNA solution was injected into each egg within 2–3 h after oviposition (Yamaguchi et al., 2011). The injected embryos were incubated at 25 °C in a humidified Petri dish until hatching. Injected individuals were crossed with non-injected individuals to obtain G_1 broods. We screened them by T7 endonuclease I (T7ENI) assay (for detail, see below) and identified G_1 broods in which mutant alleles were transmitted from G_0. We maintained the screened broods and established the mutant line according to the mating scheme reported by Daimon et al. (2014).

2.3. Expression MascR-EGFP fusion protein in cultured cells

The *Fem* piRNA-resistant Masc (Masc-R)-EGFP expression plasmid was constructed as reported previously (Sugano et al., 2016). Plasmid mutagenesis was performed using a KOD-Plus-Mutagenesis Kit (TOYOBO) with the primers listed in Supplemental Table S1. To enhance the translation level of the Masc protein, 10-bp 5′ untranslated region was added to the *Masc* coding sequence. DNA sequences were verified using an ABI Prism 3100 DNA sequencer (Applied Biosystems). *B. mori* embryo-derived NIAS-Bm-M1 (M1) cells (Suzuki et al., 2008) were cultured at 27 °C in TC-100 medium supplemented with 10% fetal bovine serum. M1 cells (4×10^5 cells per 35-mm diameter dish) were transfected with plasmid DNAs (1 μg) using X-tremeGENE HP (Roche). Three days after transfection, EGFP fluorescence was observed and captured using Floid Cell Imaging Station (Invitrogen).

2.4. Immunoprecipitation and immunoblotting

Anti-Masc rabbit polyclonal antibody was produced using mixed synthetic peptides (Pos: 20–36 and 281–300) as antigens (Sigma-Aldrich). To detect Masc protein *in vivo*, three pairs of testes were collected from day 3 fifth instar larvae and homogenized in buffer attached with LysoPure™ Nuclear and Cytoplasmic Extractor Kit (Wako). Nuclear insoluble fraction was obtained in accordance with the manufacturer's protocol and used for SDS-PAGE, followed by immunoblotting with anti-Masc antibody.

M1 cells transfected with *Masc* cDNAs were immunoprecipitated with anti-GFP beads using μMACS GFP Tagged Protein Isolation Kit (Miltenyi Biotec). Immunoprecipitated proteins were eluted from the beads under a nondenaturing condition and subjected to SDS-PAGE. Immunoblotting was performed with anti-GFP polyclonal antibody (MBL).

2.5. T7ENI cleavage assay

Genomic DNA was extracted using the hot sodium hydroxide and tris (HotSHOT) method (Truett et al., 2000). PCR was conducted using *TaKaRa Ex Taq*® (TaKaRa) under the following conditions: 94 °C for 2 min; 40 cycles of 94 °C for 30 s, 60 °C for 30 s, and 72 °C for 30 s, followed by 72 °C for 5 min. The PCR product was annealed under the following conditions: 95 °C for 10 min, 85 °C for 1 min, 75 °C for 1 min, 65 °C for 1 min, 55 °C for 1 min, 45 °C for 1 min, 35 °C for 1 min, and 25 °C for 1 min, followed by 4 °C. The annealed PCR products were cleaved by T7ENI (NEB) at 37 °C for 1 h. The cleavage products were detected by agarose gel electrophoresis. The primers used for the T7ENI cleavage assay are listed in Supplemental Table S1.

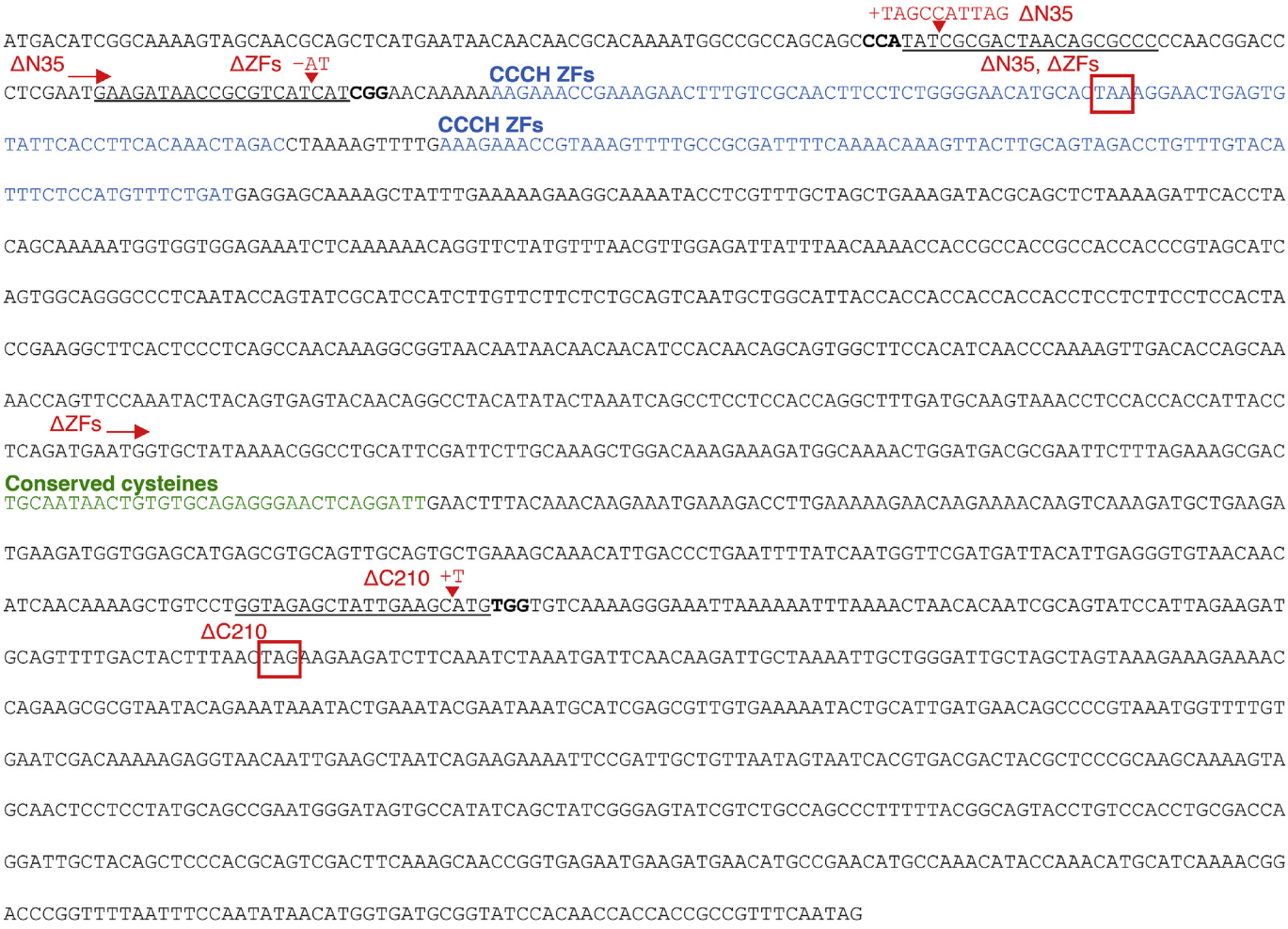

Fig. 1. CRISPR/Cas9-introduced mutations in the *Masc* coding sequence. The target sequences of sgRNAs are indicated by *underlining*. Proto-spacer adjacent motifs (PAMs) are highlighted in *bold*. Cleavage sites are shown by *arrowheads*. The deleted (−) and inserted (+) sequences are shown on the cleavage sites. Predicted initiation codons in *Masc* mutant strains are indicated by *arrows*. Premature stop codons caused by the mutations are highlighted by *squares*. The *blue* and *green letters* indicate the locations of two CCCH-type zinc finger domains (ZFs) and highly conserved region containing two cysteine residues, respectively. Transcription of each mutant *Masc* mRNA was confirmed by cDNA sequencing. (For interpretation of the references to color in this figure legend, the reader is referred to the Web version of this article.)

2.6. Molecular sexing

Genomic DNA was extracted from an embryo, a newly hatched larva, and a middle leg of an adult moth using the HotSHOT method. Genomic DNA was also prepared from a single embryo used in total RNA extraction using TRIzol reagent (Invitrogen), in accordance with the manufacturer's protocol. Molecular sexing was carried out by genomic PCR using KOD FX Neo (TOYOBO) with a W-specific marker, *Musashi*, under the following conditions: 94 °C for 2 min; 40 cycles of 98 °C for 10 s, 52 °C for 30 s, and 68 °C for 1.5 min; followed by 68 °C for 2 min (Kiuchi et al., 2014). Molecular sexing was also performed by quantitative reverse transcription-PCR (RT-qPCR) analysis using a W-

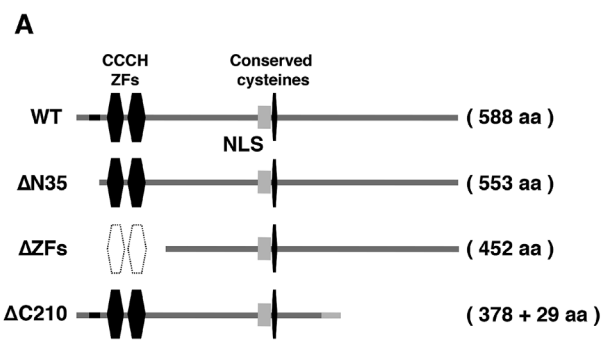

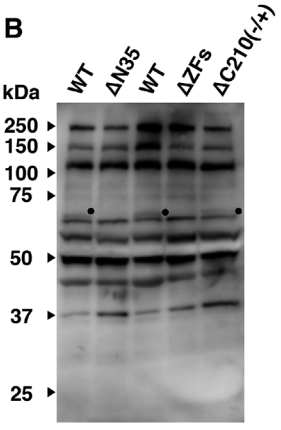

Fig. 2. The Masc proteins produced in the mutant strains. *A*, Domain structure of the Masc protein in the mutant strains. The *hexagons* indicate the location of two CCCH-type zinc finger domains (ZFs) and a highly conserved region containing two cysteine residues. The nuclear localization signal (NLS) is indicated by a *light gray box*. Deleted ZFs are shown by a *dashed line*. The recognition site of anti-Masc antibody in the N-terminus and the extra amino acids in the C-terminus are shown by *black* and *light gray bars*, respectively. *B*, Detection of the Masc proteins. Testicular proteins were separated by SDS-PAGE and immunoblotted with anti-Masc polyclonal antibody. The Masc proteins are indicated by *dots*. Numbers to the left indicate the positions of molecular weight markers (kDa).

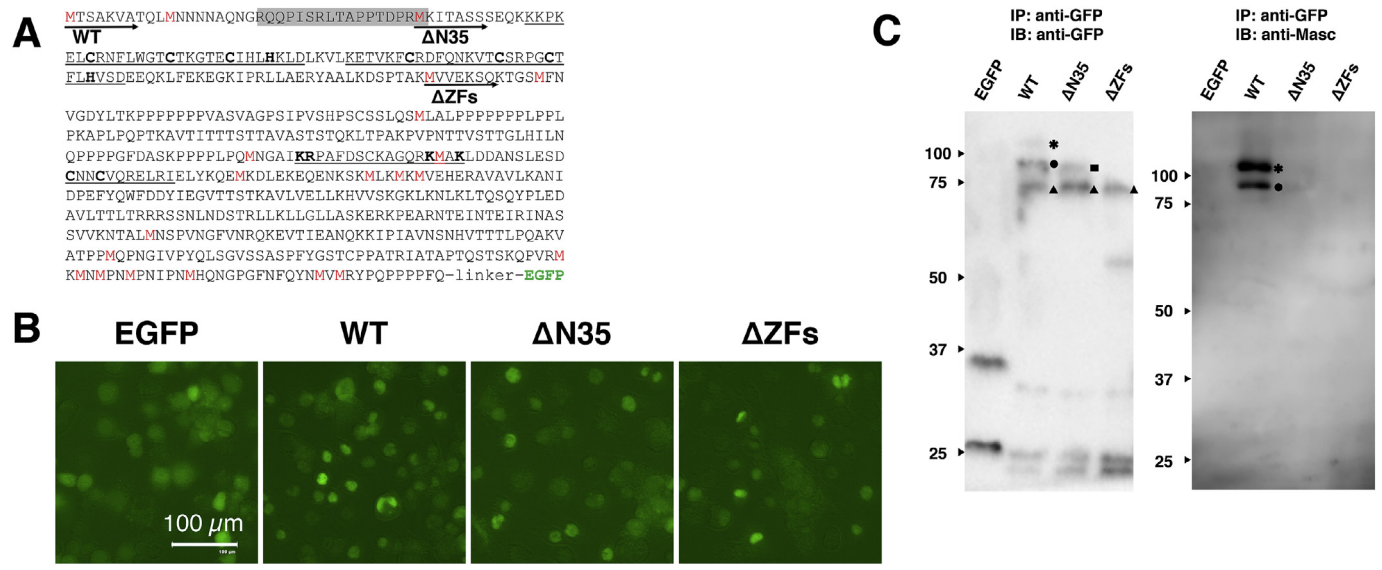

Fig. 3. Expression of the N-terminally truncated Masc protein in *B. mori* cultured cells. *A*. Amino acid sequence of EGFP-fused Masc-R proteins. Methionine residues and predicted translation start sites are indicated by *red letters* and *arrows*, respectively. The synthetic peptide sequence in the N-terminus is highlighted in *gray*. Two CCCH-type zinc finger domains, nuclear localization signal, and highly conserved region containing two cysteine residues are indicated by *underlining*. The conserved CCCH residues, essential basic amino acid residues for nuclear localization, and two cysteine residues required for masculinizing activity are shown in *bold*. *B*. Expression of EGFP-fused Masc-R proteins in M1 cells. The wild-type and N-terminally truncated Masc-R proteins fused to EGFP were localized to the nucleus of M1 cells. *C*. Immunodetection of EGFP-fused Masc-R proteins. EGFP-fused Masc-R proteins were immunoprecipitated (IP) with anti-GFP antibody, and then immunoblotted (IB) with the indicated antibodies. The EGFP-fused Masc-R proteins (WT) and their dimers are indicated by *dots* and *asterisks*, respectively. The ΔN35- and ΔZF-type Masc-R proteins fused to the EGFP are indicated by a *square* and *triangles*, respectively. Numbers to the left indicate the positions of molecular weight markers (kDa). (For interpretation of the references to color in this figure legend, the reader is referred to the Web version of this article.)

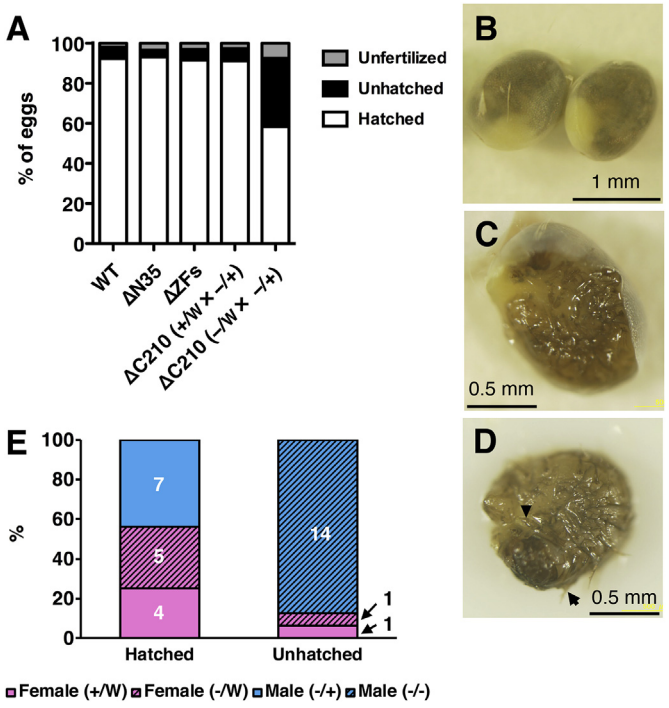

Fig. 4. Effect of the *Masc* mutation on hatchability. *A*, Hatching rate of the *Masc* mutant strains. The percentages of hatched and unhatched eggs are indicated by *white* and *black bars*, respectively. The ratio of unfertilized eggs is represented by *gray bars*. The crossing patterns are indicated in brackets. The raw data are shown in Table 3. *B*, An image of unhatched male embryos in the ΔC210 strain (−/−). *C–D*, The dead larva in the egg shell. The *arrowhead* indicates foreleg and the *arrow* indicates dorsal hair. *E*, Genotyping of embryos in the ΔC210 strain. The sex of individual embryos was determined by PCR of a W-chromosome-specific marker and the genotypes shown in brackets were determined by DNA sequencing. The number indicates the sample size.

specific marker, *Fem*. The oligonucleotide sequences of W-specific markers are listed in Supplemental Table S1.

2.7. Genotyping

Genotyping of *Masc* mutant strains was performed by T7ENI cleavage assay or DNA sequencing with BigDye® Terminator v3.1 Cycle Sequencing Kit (Applied Biosystems) and ABI PRISM® 3130*xl* Genetic Analyzer (Applied Biosystems). The primers are listed in Supplemental Table S1.

2.8. RT-PCR

Total RNA was prepared from an embryo using TRIzol reagent in accordance with the manufacturer's protocol and subjected to reverse transcription using avian myeloblastosis virus reverse transcriptase with an oligo-dT primer (TaKaRa). RT-PCR was conducted using KOD FX Neo under the following conditions: 94 °C for 2 min; 40 cycles of 98 °C for 15 s, 60 °C for 30 s, and 68 °C for 30 s; followed by 68 °C for 2 min. Splicing patterns of *Bmdsx* were examined by RT-PCR with the primers listed in Supplemental Table S1. RT-qPCR was performed using KAPA™ SYBR FAST qPCR kit (KAPA Biosystems) and StepOnePlus™ Real-Time PCR System (Applied Biosystems). The gene-specific primers are listed in Supplemental Table S1. *Masc* cDNAs from mutant strains for DNA sequencing were obtained by RT-PCR using KOD One (TOYOBO) with the primers listed in Supplemental Table S1 under following conditions: 40 cycles of 98 °C for 10 s, 60 °C for 5 s, and 68 °C for 10 s.

3. Results

3.1. Establishment of Masc mutant strains by CRISPR/Cas9 system

The *Masc* gene is located on the Z chromosome and consists of ten exons and nine introns (Kiuchi et al., 2014). We designed three sg RNAs

for targeting different positions of the *Masc* gene (Fig. 1). We injected them with *Cas9* mRNA into newly laid eggs and successfully introduced an insertion or a deletion into the exons of the *Masc* gene. All insertions or deletions caused premature stop codons, resulting in the production of N- or C-terminally truncated Masc proteins. The predicted structures of these truncated Masc proteins produced in the three established mutant strains are shown in Fig. 2A. The ΔN35 strain had a 10-bp insertion in exon 2 and potentially produced N-terminally truncated Masc protein. ΔZFs is a strain lacking both of the two ZFs by a 2-bp deletion in exon 2. The ΔC210 strain lacked a large part of the C-terminal region but retained two conserved cysteine residues required for the masculinizing activity. This mutated Masc protein also contained 29 unrelated amino acids at the C-terminus.

3.2. Production of truncated Masc proteins in Masc mutant strains

To detect Masc proteins produced in *Masc* mutant strains, we produced anti-Masc polyclonal antibody using two synthetic peptides (N-terminus and a middle part of the Masc sequence) as antigens. However, the antibody recognized only the N-terminal region of the Masc protein (Fig. 2B). Although many non-specific bands were detected in all testicular samples, a 64 kDa band was specifically obtained in wild-type and ΔC210 (−/+) strains (dots in Fig. 2B). The corresponding band was not detected in ΔN35 and ΔZFs strains. The C-terminally truncated Masc protein was not detected in the male larvae carrying the heterozygous mutation (−/+) in ΔC210 strain. To verify the production of N-terminally truncated Masc protein in ΔN35 and ΔZFs strains, we constructed expression plasmids that express the Masc-R or ΔN35- and ΔZF-type Masc-R proteins fused to the enhanced green fluorescent protein. The predicted amino acid sequences are shown in Fig. 3A. In ΔN35 strain, the N-terminally truncated Masc-R-EGFP protein is predicted to be translated from the 3rd methionine. On the other hand, two ZFs are predicted to be lost in ΔZFs strain by translation from the 4th methionine. All N-terminally truncated Masc-R-EGFP proteins were produced and localized to the nucleus of *B. mori* embryonic cultured cell line, M1 (Fig. 3B). Production of the EGFP-fused, N-terminally truncated Masc proteins in M1 cells was verified by immunoblotting of the immunoprecipitated proteins (Fig. 3C), indicating that the N-terminally truncated Masc-R-EGFP proteins were also translated in *B. mori* cells. The ΔZF-type Masc-R proteins fused to the EGFP were also translated in cells transfected with the wild-type and the ΔN35-type plasmids (Fig. 3C).

3.3. Sex differentiation of Masc mutant strains

We maintained three *Masc* mutant strains with fresh mulberry leaves and sexed individual animals at the pupal stage. No apparent abnormality was observed in the pupae of all mutant strains. We distinguished between males and females by looking at the 9th and 8th abdominal segments of the pupae, respectively, and found that the ratio of male to female pupae was approximately 50% in all mutant strains, except for in the ΔC210 strain (Table 1). When a female moth carrying the mutation (−/W) was crossed with a male moth carrying the heterozygous mutation (−/+) in the ΔC210 strain, the proportion of male pupae decreased (Tukey's wholly significant difference test, $p < 0.05$). Molecular sexing using a W-chromosome-specific marker revealed that sex reversal did not occur in any mutant strains (Table 2). Mutant female progeny (−/W) were normally obtained from the male parents carrying a heterozygous mutation (−/+) in both the ΔZFs and ΔC210 strains (Table 2). We obtained male moths carrying a homozygous mutation in ΔN35 and ΔZFs, but not in ΔC210, indicating that ΔC210 (−/−) is lethal in males. No external morphological abnormalities were observed at the adult stage in all mutant strains (results not shown).

Table 1
The sex ratio of the *Masc* mutant pupae.

Strain	No. of female pupae (%)	No. of male pupae (%)	Total
WT	31 (48.4)	33 (51.6)	64
	47 (54.7)	39 (45.3)	86
	59 (50.9)	57 (49.1)	116
ΔN35	67 (54.9)	55 (45.1)	122
	62 (57.9)	45 (42.1)	107
	48 (51.1)	46 (48.9)	94
ΔZFs	45 (48.4)	48 (51.6)	93
	58 (48.7)	61 (51.3)	119
	44 (46.8)	50 (53.2)	94
ΔC210 (+/W × −/+)	52 (43.7)	67 (56.3)	119
	69 (53.1)	61 (46.9)	130
	45 (48.9)	47 (51.1)	92
ΔC210 (−/W × −/+)	64 (66.0)	33 (34.0)	97
	62 (63.3)	36 (36.7)	98
	60 (65.2)	32 (34.8)	92

3.4. Fertility and hatchability of Masc mutant strains

In ΔN35 and ΔZFs strains, female moths mated with male moths normally and laid enough eggs (approximately 200 eggs/moth, Table 3). Almost all embryos developed normally and hatched at 10 days postoviposition (Fig. 4A). The male moths carrying the heterozygous mutation (−/+) in ΔC210 were appreciably attracted to both the wild type (+/W) and the mutant female moths (−/W) and then mated with them. Most embryos from the wild-type (+/W) females developed normally, while approximately 30% of embryos from the ΔC210 (−/W) females died at 1 day before hatching (Fig. 4A and B, Table 3). We dissected the dead ΔC210 embryos and observed normally colored larval bodies with legs and hairs (Fig. 4C and D). Most of the unhatched embryos were males with the homozygous mutation (−/−) (Fig. 4E). In addition, we did not find males carrying the homozygous mutation (−/−) in newly hatched larvae, indicating that ΔC210 (−/−) is embryonic lethal in males.

3.5. Expression of the sex-determining genes in Masc mutant strains

To examine the effect of the *Masc* mutation on sexual differentiation, we investigated *Bmdsx* splicing and *BmImp*^{M} expression in molecularly sexed embryos. In most cases, genetically defined sexes were identical to those of the patterns of *Bmdsx* splicing and *BmImp*^{M} expression. However, ΔC210 (−/−) male embryos expressed the female-type isoform of *Bmdsx* and did not exhibit *BmImp*^{M} expression (Fig. 5A and B). In both sexes, the *Masc* mRNA levels in ΔZFs and ΔC210 (both genotypes) embryos were comparable to those in wild-type embryos (Fig. 5C). In addition, male-biased expression of the *Masc* gene was also observed in mutant embryos, suggesting that mutant *Masc* mRNAs are normally expressed in terms of the mRNA level and expression pattern. These results indicate a defect of masculinization in ΔC210 (−/−) male embryos.

3.6. Dosage compensation in Masc mutant strains

To investigate whether dosage compensation is normally established in mutant strains, we measured the expression levels of Z-linked genes in wild-type and mutant embryos (Fig. 6). We performed RT-qPCR experiments of five genes (*BGIBMGA002078*, *BGIBMGA003860*, *BGIBMGA000710*, *BGIBMGA012270*, and *BGIBMGA000486*) that were selected from various positions of the Z chromosome (Table S1). The results clearly showed that the expression levels of all examined Z-

Table 2
Molecular sexing and genotyping of the *Masc* mutant moths.

Strain	♀			♂			
	+/W[a] (%)	−/W (%)	Total	+/+ (%)	−/+ (%)	−/− (%)	Total
ΔN35 (−/W × −/−)	0	6 (100)	6	0	0	6 (100)	6
ΔZFs (−/W × −/+)	6 (50.0)	6 (50.0)	12	0	6 (50.0)	6 (50.0)	12
ΔC210 (+/W × −/+)	6 (50.0)	6 (50.0)	12	6 (50)	6 (50.0)	0	12
ΔC210 (−/W × −/+)	6 (50.0)	6 (50.0)	12	0	12 (100)	0	12

[a] The sex of individual moth was determined by PCR of the W-chromosome-specific marker and the genotypes were determined by T7ENI assay or DNA sequencing.

Table 3
Hatchability of the *Masc* mutant strains.

Strain	No. of hatched eggs (%)	No. of unhatched eggs (%)	No. of unfertilized eggs (%)	Total
WT	158 (90.8)	14 (8.0)	2 (1.1)	174
	204 (91.9)	14 (6.3)	4 (1.8)	222
	196 (94.2)	6 (2.9)	6 (2.9)	208
ΔN35	177 (95.7)	6 (3.2)	2 (1.1)	185
	176 (91.2)	5 (2.6)	12 (6.2)	193
	183 (92.9)	8 (4.1)	6 (3.0)	197
ΔZFs	127 (84.1)	17 (11.3)	7 (4.6)	151
	216 (93.1)	6 (2.6)	10 (4.3)	232
	185 (97.4)	5 (2.6)	0 (0)	190
ΔC210 (+/W × −/+)	193 (90.6)	14 (6.6)	6 (2.8)	213
	212 (90.2)	18 (7.7)	5 (2.1)	235
	139 (92.7)	7 (4.7)	4 (2.7)	150
ΔC210 (−/W × −/+)	71 (53.8)	47 (35.6)	14 (10.6)	132
	174 (69.3)	68 (27.1)	9 (3.6)	251
	98 (52.1)	75 (39.9)	15 (8.0)	188

linked genes were comparable between the wild-type and ΔZFs strains. On the other hand, ΔC210 (−/−) male embryos expressed Z-linked genes at levels more than twice as high as the wild type. The expression level of an autosomal gene, *BGIBMGA009017*, was comparable among both sexes of all strains. These results clearly showed that dosage compensation was established in ΔZFs (−/−) males, but not in ΔC210 (−/−) males.

4. Discussion

4.1. In vivo characterization of mutant Masc proteins

The Masc protein has been shown to play essential roles in masculinization and dosage compensation in *B. mori*, but it is largely unknown how this protein functions separately in each context. In cell-based assays using *B. mori* cultured cells, we have revealed that two conserved cysteine residues (Cys-301 and Cys-304) are essential for masculinization, but two CCCH-type ZFs are not (Katsuma et al., 2015). As our assay system was considered inappropriate for assessing Z-linked gene expression, it is necessary to establish a novel system to evaluate dosage compensation when the Masc protein is modified. To determine the critical region required for dosage compensation and to understand the mechanism by which Masc protein accomplishes this process, we attempted to generate mutant silkworms in which the *Masc* gene is partially deleted. Using these mutant strains, we investigated which regions are involved in dosage compensation or sexual differentiation *in vivo*.

To examine the production of the truncated Masc proteins instead of the wild-type one in each mutant strain, we generated anti-Masc polyclonal antibody using synthetic peptides. The antibody seemed to recognize the N-terminal region of the Masc protein. As shown in Fig. 2B, a specific 64 kDa band was detected in wild-type and ΔC210 (−/+) testes. The C-terminally truncated Masc protein (presumed molecular weight is 45 kDa) was not detected in ΔC210 (−/+) strains. This was presumably because large C-terminal deletion affected the stability of the protein. On the other hand, no specific bands were detected in ΔN35 and ΔZFs strains since Masc proteins produced in these strains lacked the antibody epitope (Fig. 2A). As the phenotypes of these strains were indistinguishable from that of wild-type strain, the N-terminally truncated proteins ought to be produced in ΔN35 and ΔZFs strains. Expression analysis in *B. mori* cultured cells strongly supported the translation from the internal initiation codons in these mutant Masc proteins (Fig. 3B and C).

4.2. The role of CCCH-type zinc finger domains in the Masc protein

Unexpectedly, the strain lacking both of the two CCCH ZFs (ΔZFs) did not show any defective phenotypes at any developmental stages, indicating that Masc's ZFs are not required for sexual differentiation and dosage compensation. We previously found that Masc orthologue in *Trilocha varians* (Bombycidae) exhibits masculinizing activity, regardless of the absence of two amino acid residues between the conserved second and third cysteine residues in its second CCCH ZF (Fig. S1). This result also supports our conclusion. However, two CCCH ZFs are highly conserved among lepidopteran insects in spite of the overall low sequence homology of Masc homologs (Fig. S1) (Katsuma et al., 2015). What is the role of Masc's ZFs? The CCCH-type ZF-containing proteins usually function by binding DNA or RNA in cells (Pomeranz et al., 2010; Brooks and Blackshear, 2013; Blackshear and Perera, 2014). Masc ZFs are not essential, but might have positive effects on the transcriptional repression of Z-linked genes via assisting Masc's binding to nucleic acids. We are currently investigating this possibility.

Another possibility explaining the lack of defective phenotypes in ΔZFs silkworms is that the loss of Masc ZFs could be functionally compensated for by other ZF-containing proteins, such as BmZNF-2 (BGIBMGA004989) (Gopinath et al., 2016). BmZNF-2 is a recently discovered protein that also possesses two tandemly arranged CCCH ZFs in the N-terminus and two cysteine residues in the central region (Fig. S1). However, some of the residues within the highly conserved 11-amino-acid region are not identical to those of Masc homologs (Fig. S1). Our previous study revealed that amino acid substitution of some of these residues reduced the masculinizing activity but did not abolish it completely (Katsuma et al., 2015). Gopinath et al. reported that transfection of *Bmznf-2* cDNA into BmN-4 cells induced $Bmdsx^{M}$ expression (Gopinath et al., 2016), suggesting that the product of this gene possesses masculinizing activity in *B. mori* cells. Although the *in vivo* functions of BmZNF-2 protein remain unknown, it is likely that this protein could compensate for the loss of Masc ZF functions in ΔZFs animals.

4.3. The effects of Masc deletion on male development

Homozygous deletion of the 210 C-terminus amino acids resulted in

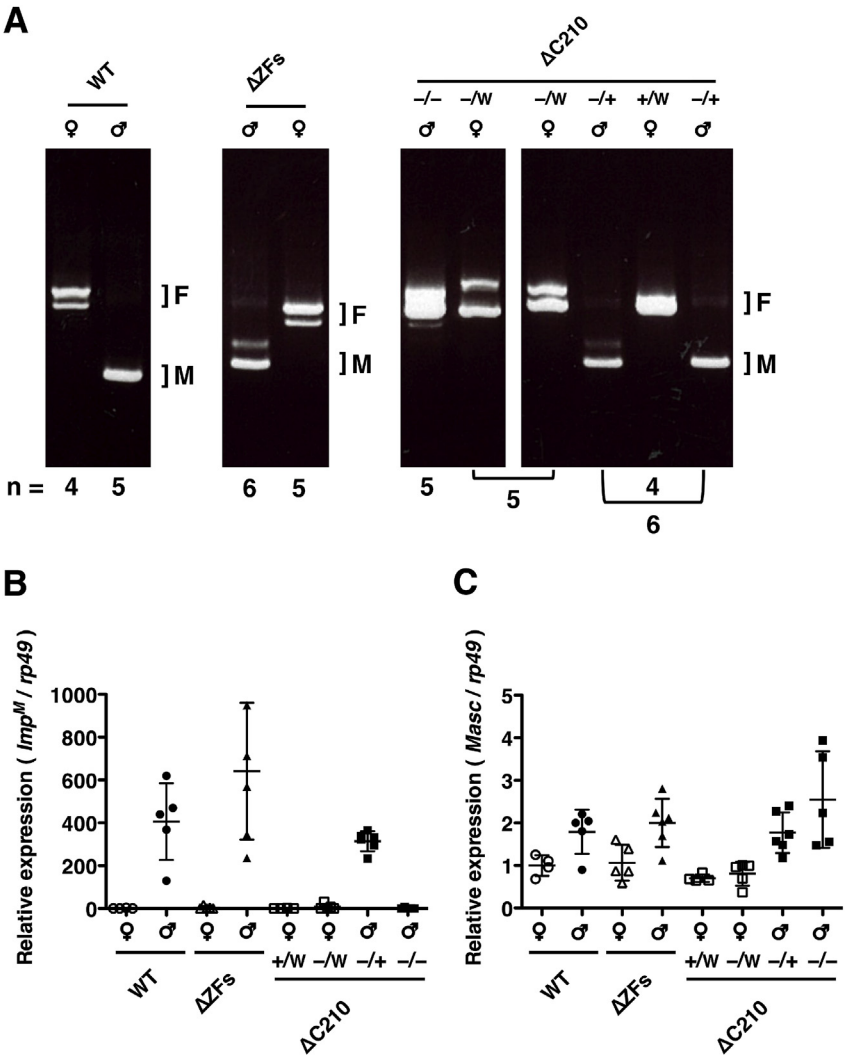

Fig. 5. Effect of the *Masc* mutation on the expression of the sex-determining genes. *A*, Representative splicing pattern of *Bmdsx* in early embryos (72 hpo) of the *Masc* mutant strains. The *Bmdsx* splicing was examined by RT-PCR. The molecular sex of the embryos was determined by PCR and RT-qPCR of W-chromosome-specific markers. The F and M indicate female- and male-type splicing of *Bmdsx*, respectively. The number indicates the sample size. *B–C*, Expression of the masculinizing genes in early embryos. The expression levels of $BmIMP^{M}$ and *Masc* were examined by RT-qPCR. The relative mRNA levels (wild-type female = 1) were normalized to that of *rp49*. The bars indicate means ± SD. The sample size is the same as in Fig. 5A.

an embryonic lethal phenotype only in males (Fig. 4E). This defect is presumably caused by the abnormal transcriptional upregulation of Z-linked genes in male embryos (Fig. 6). Similar results were obtained when *Masc* mRNA was transiently knocked down by injecting *Masc* siRNA into *B. mori* embryos (Kiuchi et al., 2014). However, in embryonic RNAi experiments, it was difficult to evaluate the precise timing of individual death owing to many factors, including the difference in knockdown efficiency and endurance among the embryos. In the present study, we dissected unhatched male embryos of ΔC210 (−/−) and observed that larval bodies were completely developed and colored normally, but they did not move at all (Fig. 4B–D). This clearly showed that the failure of dosage compensation does not affect embryogenesis in *B. mori*. Similar phenomenon was also observed in *Drosophila melanogaster*. Although dosage compensation begins at early embryogenesis in *D. melanogaster*, mutations in the dosage compensation regulators cause male-specific lethality during the late larval or early pupal stages (Belote and Lucchesi, 1980; Rastelli et al., 1995; Franke et al., 1996).

The Masc protein produced in ΔC210 lacks a large part of the C-terminal region but possesses the highly conserved region required for masculinization *in vitro* (Fig. 2A) (Katsuma et al., 2015). However, ΔC210 males with homozygous mutation (−/−) lost the masculinizing activity and the compensation of Z-linked gene dosage (Fig. 5A and B, and 6). Immunoblotting with anti-Masc antibody showed loss or very low abundance of the ΔC210 Masc protein in mutant testis, suggesting that loss-of-function of this strain results from low abundance but not from functional disruption of the Masc protein. In our cell-based assays, we found that the Masc derivative lacking the 294 N-terminal amino acids possessed the masculinizing activity, but further deletion of the C-terminal region from this derivative completely abolished it (Katsuma et al., 2015). As no other conserved regions in lepidopteran Masc homologs were detected (Fig. S1) (Katsuma et al., 2015), it was speculated that the C-terminal region might be required for the stability and/or precise conformation of the Masc protein, which is a major reason for low abundance and/or instability of the ΔC210 Masc protein.

Silkworms with heterozygous deletion of the 210 C-terminal amino acids [ΔC210 (−/+)] did not exhibit any defects in sexual differentiation and transcription of Z-linked genes when compared with the wild type (Figs. 5 and 6). In *B. mori*, *Masc* mRNA level is controlled by the W-chromosome-derived female-specific piRNA in females, whereas how *Masc* mRNA is regulated in males is unknown. Immunoblotting showed that Masc protein are sufficiently expressed in males carrying the heterozygous mutation (−/+) in ΔC210 strain compared to wild-type strain (Fig. 2B). Our study suggests that one intact *Masc* allele is sufficient for silkworm male development. In lepidopteran species that are monosomic (Z0) in females and ZZ in males, the number of Z chromosomes is believed to be the important sex determiner (Traut et al., 2007). If *Masc* is also involved in sex determination and dosage compensation in Z0/ZZ moths, the transcriptional regulation of *Masc* is more crucial than that in *B. mori* because they do not possess female-specific factors for controlling *Masc* mRNA levels.

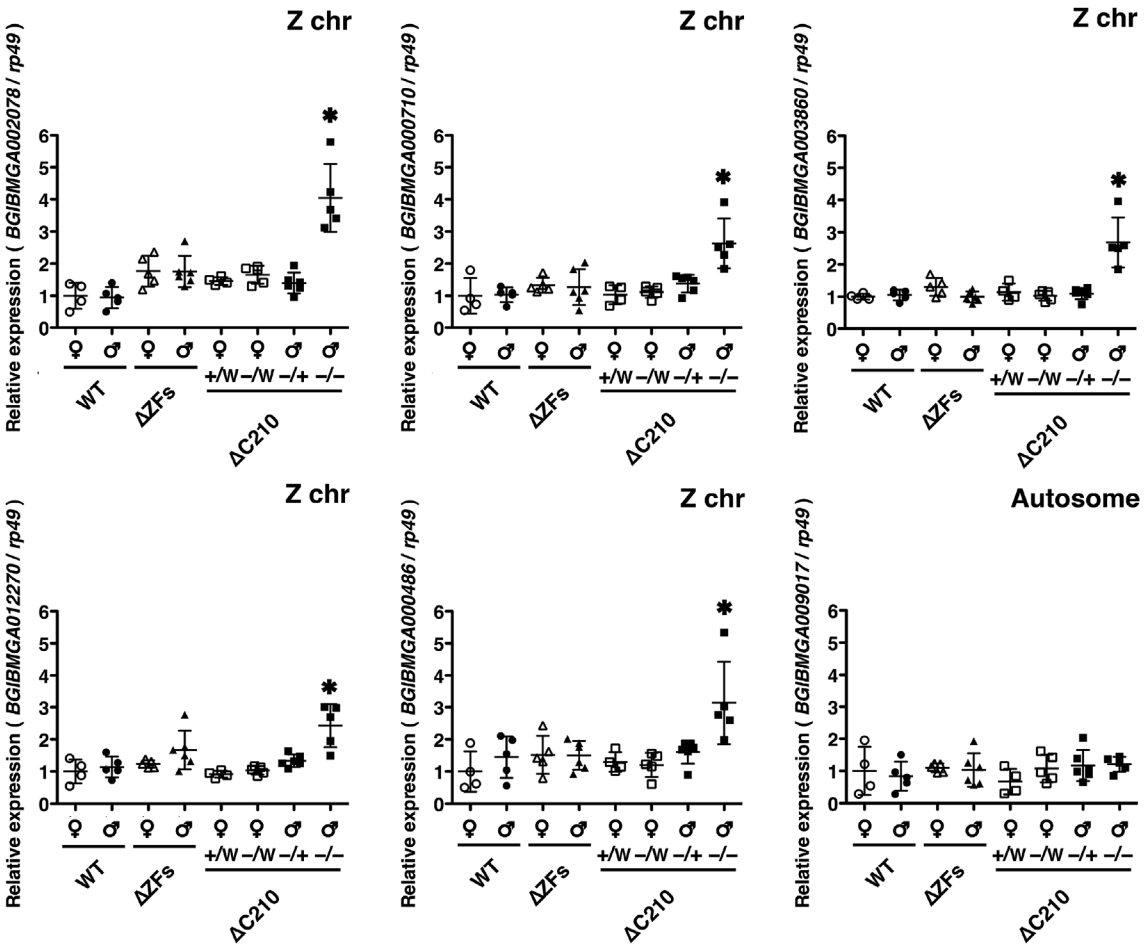

Fig. 6. Effect of the *Masc* mutation on dosage compensation. The expression levels of five Z-linked genes and one autosomal gene were examined by RT-qPCR in the early embryonic stage (72 hpo). The relative expression levels (wild-type female = 1) were normalized to that of *rp49*. The molecular sex of the embryos was determined by PCR and RT-qPCR of W-chromosome-specific markers. The bars indicate means ± SD. The sample size is the same as in Fig. 5A. *Asterisks* indicate a significant difference in one-way ANOVA with *post hoc* Tukey's test ($p < 0.05$).

4.4. The prospect of CRISPR/Cas9-mediated mutagenesis in the Masc gene

The CRISPR/Cas9 system has been shown to be applicable to a wide range of organisms including insects (Bassett et al., 2013; Awata et al., 2015). Gene knockout *B. mori* has been generated using this genome editing tool (Wang et al., 2013; Daimon et al., 2014; Ma et al., 2014; Wei et al., 2014), but there have been no reports on the generation of a series of different alleles of a single gene. In the present study, we used three different sgRNAs for targeting the *Masc* gene (Fig. 1), and successfully established three mutant strains, ΔN35, ΔZFs, and ΔC210. All of the Masc proteins produced in each mutant possess the highly conserved cysteines at residues 301 and 304 in the central region but lack partially N- or C-terminal region (Fig. 2A). Using these mutant strains, we showed that two ZFs of the Masc protein are not required for sexual differentiation and dosage compensation. On the other hand, we were not able to narrow down the region(s) required for masculinization and dosage compensation precisely. This is mainly because the target specificity of Cas9 restricts the cleavage positions of the gene of interest and we selected only three appropriate sites in the *Masc* gene. Recently, several attempts to expand the targetable sequences in Cas9-mediated genome editing applications have been reported (Hirano et al., 2016; Zeng et al., 2016). Furthermore, new editing methods using other endonucleases, such as Cpf1, have been developed (Yamano et al., 2016). Using such newly developed genome editing tools, we will be able to generate more *Masc* mutant strains and thereby explore the detailed mechanisms by which the Masc protein controls the dual biological processes of masculinization and dosage compensation.

Author contributions

TK and SK designed the study. TK conducted most of the experiments. YS and SK detected the Masc proteins using immunological methods and cell-based assays. TK and SK analyzed the data and wrote the manuscript with intellectual input from all authors. TS reviewed the manuscript and gave suggestions for improvement.

Conflicts of interest

The authors declare that they have no conflicts of interest with the contents of this article.

Acknowledgments

We thank Munetaka Kawamoto for clerical assistance and Masaru Fujimoto for technical suggestions. We also thank the Institute for Sustainable Agro-ecosystem Services, the University of Tokyo, for facilitating the mulberry cultivation. NIAS-Bm-M1 cells were provided by the National Institute of Agrobiological Sciences. Some experiments were done in Biotron Facility at the University of Tokyo. This work was supported by the Program for Promotion of Basic and Applied Researches for Innovations in Bio-oriented Industry (grant number 26034A) to SK, JSPS KAKENHI (grant number 15H02482) to TK, TS,

and SK, and MEXT KAKENHI (grant number 17H06431) to TK and SK.

Appendix A. Supplementary data

Supplementary data to this article can be found online at https://doi.org/10.1016/j.ibmb.2018.12.003.

References

Awata, H., Watanabe, T., Hamanaka, Y., Mito, T., Noji, S., Mizunami, M., 2015. Knockout crickets for the study of learning and memory: dopamine receptor Dop1 mediates aversive but not appetitive reinforcement in crickets. Sci. Rep. 5, 15885.

Bassett, A.R., Tibbit, C., Ponting, C.P., Liu, J.-L., 2013. Highly efficient targeted mutagenesis of *Drosophila* with the CRISPR/Cas9 system. Cell Rep. 4, 220–228.

Belote, J.M., Lucchesi, J.C., 1980. Male-specific lethal mutations of *Drosophila melanogaster*. Genetics 96, 165–186.

Blackshear, P.J., Perera, L., 2014. Phylogenetic distribution and evolution of the linked RNA-binding and NOT1-binding domains in the tristetraprolin family of tandem CCCH zinc finger proteins. J. Interferon Cytokine Res. 34, 297–306.

Brooks, S.A., Blackshear, P.J., 2013. Tristetraprolin (TTP): interactions with mRNA and proteins, and current thoughts on mechanisms of action. Biochim. Biophys. Acta (BBA)-Gene Regul. Mech. 1829, 666–679.

Daimon, T., Kiuchi, T., Takasu, Y., 2014. Recent progress in genome engineering techniques in the silkworm, *Bombyx mori*. Dev. Growth Differ. 56, 14–25.

Franke, A., Dernburg, A., Bashaw, G.J., Baker, B.S., 1996. Evidence that MSL-mediated dosage compensation in *Drosophila* begins at blastoderm. Development 122, 2751–2760.

Fukui, T., Kawamoto, M., Shoji, K., Kiuchi, T., Sugano, S., Shimada, T., Suzuki, Y., Katsuma, S., 2015. The endosymbiotic bacterium *Wolbachia* selectively kills male hosts by targeting the masculinizing gene. PLoS Pathog. 11, e1005048.

Gopinath, G., Arunkumar, K.P., Mita, K., Nagaraju, J., 2016. Role of *Bmznf-2*, a *Bombyx mori* CCCH zinc finger gene, in masculinisation and differential splicing of *Bmtra-2*. Insect Biochem. Mol. Biol. 75, 32–44.

Hasimoto, H., 1933. The role of the W-chromosome in the sex determination of *Bombyx mori*. Jpn. J. Genet. 8, 245–247.

Hirano, S., Nishimasu, H., Ishitani, R., Nureki, O., 2016. Structural basis for the altered PAM specificities of engineered CRISPR-Cas9. Mol. Cell 61, 886–894.

Hwang, W.Y., Fu, Y., Reyon, D., Maeder, M.L., Tsai, S.Q., Sander, J.D., Peterson, R.T., Yeh, J.R.J., Joung, J.K., 2013. Efficient genome editing in zebrafish using a CRISPR-Cas system. Nat. Biotechnol. 31, 227.

Imanishi, S., Ohtsuki, Y., 1988. Characteristics of cell lines established from embryonic tissues of several races of the silkworm, *Bombyx mori*, cultured in vitro. J. Seric. Sci. Jpn. 57, 184–188.

Katsuma, S., Sugano, Y., Kiuchi, T., Shimada, T., 2015. Two conserved cysteine residues are required for the masculinizing activity of the silkworm Masc Protein. J. Biol. Chem. 290, 26114–26124.

Kiuchi, T., Koga, H., Kawamoto, M., Shoji, K., Sakai, H., Arai, Y., Ishihara, G., Kawaoka, S., Sugano, S., Shimada, T., Suzuki, Y., Suzuki, M.G., Katsuma, S., 2014. A single female-specific piRNA is the primary determiner of sex in the silkworm. Nature 509, 633–636.

Lee, J., Kiuchi, T., Kawamoto, M., Shimada, T., Katsuma, S., 2015. Identification and functional analysis of a *Masculinizer* orthologue in *Trilocha varians* (Lepidoptera: bombycidae). Insect Mol. Biol. 24, 561–569.

Ma, S., Chang, J., Wang, X., Liu, Y., Zhang, J., Lu, W., Gao, J., Shi, R., Zhao, P., Xia, Q., 2014. CRISPR/Cas9 mediated multiplex genome editing and heritable mutagenesis of *BmKu70* in *Bombyx mori*. Sci. Rep. 4, 4489.

Pomeranz, M.C., Hah, C., Lin, P.-C., Kang, S.G., Finer, J.J., Blackshear, P.J., Jang, J.-C., 2010. The *Arabidopsis* tandem zinc finger protein AtTZF1 traffics between the nucleus and cytoplasmic foci and binds both DNA and RNA. Plant Physiol. 152, 151–165.

Rastelli, L., Richman, R., Kuroda, M.I., 1995. The dosage compensation regulators MLE, MSL-1 and MSL-2 are interdependent since early embryogenesis in *Drosophila*. Mech. Dev. 53, 223–233.

Sakai, H., Sumitani, M., Chikami, Y., Yahata, K., Uchino, K., Kiuchi, T., Katsuma, S., Aoki, F., Sezutsu, H., Suzuki, M.G., 2016. Transgenic expression of the piRNA-resistant *masculinizer* gene induces female-specific lethality and partial female-to-male sex reversal in the silkworm, *Bombyx mori*. PLoS Genet. 12, e1006203.

Sander, J.D., Maeder, M.L., Reyon, D., Voytas, D.F., Joung, J.K., Dobbs, D., 2010. ZiFiT (Zinc Finger Targeter): an updated zinc finger engineering tool. Nucleic Acids Res. 38, W462–W468.

Sugano, Y., Kokusho, R., Ueda, M., Fujimoto, M., Tsutsumi, N., Shimada, T., Kiuchi, T., Katsuma, S., 2016. Identification of a bipartite nuclear localization signal in the silkworm Masc protein. FEBS Lett. 590, 2256–2261.

Suzuki, M.G., Funaguma, S., Kanda, T., Tamura, T., Shimada, T., 2005. Role of the male BmDSX protein in the sexual differentiation of *Bombyx mori*. Evol. Dev. 7, 58–68.

Suzuki, M.G., Funaguma, S., Kanda, T., Tamura, T., Shimada, T., 2003. Analysis of the biological functions of a *doublesex* homologue in *Bombyx mori*. Dev. Gene. Evol. 213, 345–354.

Suzuki, M.G., Imanishi, S., Dohmae, N., Asanuma, M., Matsumoto, S., 2010. Identification of a male-specific RNA binding protein that regulates sex-specific splicing of *Bmdsx* by increasing RNA binding activity of BmPSI. Mol. Cell Biol. 30, 5776–5786.

Suzuki, M.G., Imanishi, S., Dohmae, N., Nishimura, T., Shimada, T., Matsumoto, S., 2008. Establishment of a novel in vivo sex-specific splicing assay system to identify a trans-acting factor that negatively regulates splicing of *Bombyx mori dsx* female exons. Mol. Cell Biol. 28, 333–343.

Tanaka, Y., 1916. Genetic studies in the silkworm. J. Coll. Agric. Sapporo 6, 1–33.

Traut, W., Sahara, K., Marec, F., 2007. Sex chromosomes and sex determination in Lepidoptera. Sex. Dev. 1, 332–346.

Truett, G.E., Heeger, P., Mynatt, R.L., Truett, A.A., Walker, J.A., Warman, M.L., 2000. Preparation of PCR-quality mouse genomic DNA with hot sodium hydroxide and tris (HotSHOT). Biotechniques 29, 52–54.

Wang, Y., Li, Z., Xu, J., Zeng, B., Ling, L., You, L., Chen, Y., Huang, Y., Tan, A., 2013. The CRISPR/Cas System mediates efficient genome engineering in *Bombyx mori*. Cell Res. 23, 1414–1416.

Wei, W., Xin, H., Roy, B., Dai, J., Miao, Y., Gao, G., 2014. Heritable genome editing with CRISPR/Cas9 in the silkworm, *Bombyx mori*. PLoS One 9, e101210.

Xu, J., Chen, S., Zeng, B., James, A.A., Tan, A., Huang, Y., 2017. *Bombyx mori* P-element somatic inhibitor (*BmPSI*) is a key auxiliary factor for silkworm male sex determination. PLoS Genet. 13, e1006576.

Yamaguchi, J., Mizoguchi, T., Fujiwara, H., 2011. siRNAs induce efficient RNAi response in *Bombyx mori* embryos. PLoS One 6, e25469.

Yamano, T., Nishimasu, H., Zetsche, B., Hirano, H., Slaymaker, I.M., Li, Y., Fedorova, I., Nakane, T., Makarova, K.S., Koonin, E.V., others, 2016. Crystal structure of Cpf1 in complex with guide RNA and target DNA. Cell 165, 949–962.

Zeng, B., Zhan, S., Wang, Y., Huang, Y., Xu, J., Liu, Q., Li, Z., Huang, Y., Tan, A., 2016. Expansion of CRISPR targeting sites in *Bombyx mori*. Insect Biochem. Mol. Biol. 72, 31–40.